

Synthesis, in vitro evaluation, and SAR studies of a potential antichagasic 1*H*-pyrazolo[3,4-*b*]pyridine series

Luiza R. S. Dias,^{a,*} Marcelo B. Santos,^{a,b} Sérgio de Albuquerque,^c
Helena C. Castro,^d Alessandra M. T. de Souza,^{b,d} Antônio C. C. Freitas,^a
Maria A. V. DiVaio,^a Lucio M. Cabral^e and Carlos R. Rodrigues^e

^aUniversidade Federal Fluminense (UFF), Laboratório de Química Medicinal (LQMed), Faculdade de Farmácia,
Rua Mário Viana, 523, Santa Rosa, 24241-000, Niterói, RJ, Brazil

^bUniversidade Federal Fluminense, Instituto de Química, Departamento de Química Orgânica,

Programa de Pós-Graduação em Química Orgânica, Campus do Valonguinho, 24020-150, Niterói, RJ, Brazil

^cUniversidade de São Paulo, Departamento de Análises Clínicas, Toxicológicas e Bromatológicas, FCFRP/USP,
ZIP 29020-159, São Paulo, SP, Brazil

^dUniversidade Federal Fluminense (UFF), Laboratório de Antibióticos, Bioquímica e Modelagem Molecular (LABioMol),
Instituto de Biologia—Outeiro de São João Baptista, 24020-150, Niterói, RJ, Brazil

^eUniversidade Federal do Rio de Janeiro, Laboratório de Modelagem Molecular e QSAR (ModMolQSAR),
Faculdade de Farmácia, 21941-590, Rio de Janeiro, RJ, Brazil

Received 26 June 2006; revised 29 August 2006; accepted 29 September 2006
Available online 1 October 2006

Abstract—The development of new drugs against *Trypanosoma cruzi* is still required since the only two drugs currently used cause severe side effects. In this work we described the synthesis, the in vitro biological evaluation, and the SAR results of 1*H*-pyrazolo[3,4-*b*]pyridine derivatives, a new antichagasic agent series. The presence of fluorine, hydroxyl or nitro group at Y position resulted in at least one or two promising compounds in each set of derivatives (**6f**, **6g**, **6i**, **6l**, and **6m**). The SAR study showed that trypanocidal activity observed depends on both geometric and stereoelectronic parameters (MEP and frontier molecular orbitals HOMO and LUMO). We also used the Osiris program for calculating and comparing the fragment based druglikeness of the most active derivative (**6g**) (IC₅₀ = 1.9 µg/mL), the inactive compound (**6o**), and the current toxic antichagasic drugs (nifurtimox and benznidazole). Interestingly **6g** presented a potential druglikeness higher than nifurtimox and benznidazole while **6o** presented the lowest value among them.

© 2006 Published by Elsevier Ltd.

1. Introduction

Chagas' disease is caused by *Trypanosoma cruzi*, a parasite with a large zoonotic reservoir in Central and South America.^{1–3} Its endemic keeps 100 million people at risk and about 20 million people chronically infected with *T. cruzi*.⁴

Current treatment of Chagas' disease involves the use of nitrofurans [nifurtimox] (**1**) and nitroimidazoles [benznidazole] (**2**) (Fig. 1). However they are often poorly tolerated and may produce serious toxic effects in the host.⁴

In the acute phase of the disease, these compounds are frequently ineffective due to differences in *T. cruzi* strains' drug susceptibility, and they are useless for the chronic stage.^{5–8} Thus, effective and safe drugs are still needed for Chagas disease.

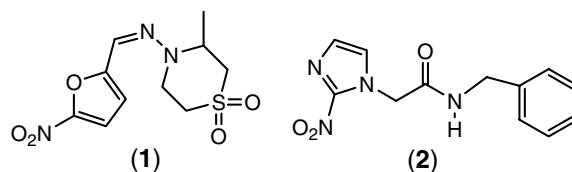
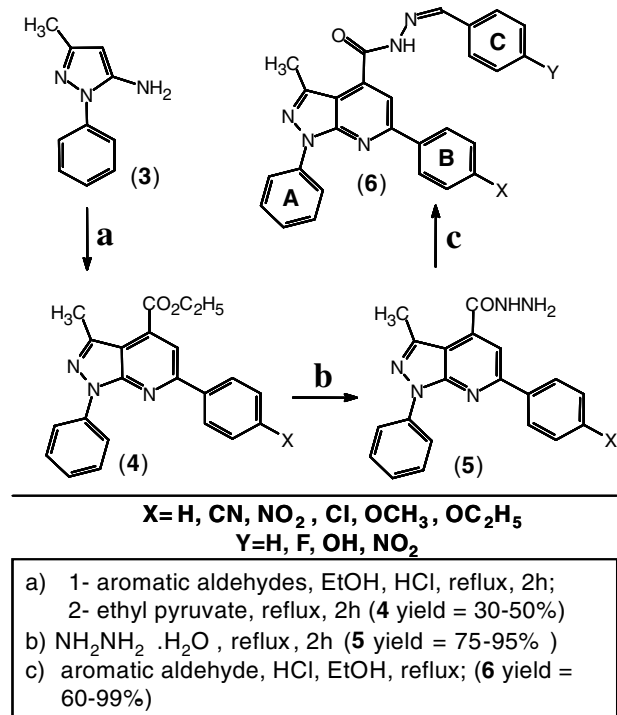


Figure 1. Nifurtimox (**1**) and benznidazole (**2**).

Keywords: Structure–activity relationship (SAR); 1*H*-pyrazolo[3,4-*b*]pyridine; Antiparasite agent; Chagas.

*Corresponding author. Tel.: +55 21 2629 9588; fax: +55 21 2629 9578; e-mail: ldias@vm.uff.br



Scheme 1. The synthetic pathway of *N'*-benzylidene-3-methyl-1,6-diphenyl-1*H*-pyrazolo[3,4-*b*]pyridine-4-carbohydrazide.

Since 1990's several phenylpyrazole derivatives have been described as antiparasites, and the nucleus 1*H*-pyrazolo[3,4-*b*]pyridine has been evaluated for its antiparasitic profile.^{9–12} Literature also described structural subunits such as carbohydrazides [R₂C = N–NH–CO–] and their importance for the antiparasitic activity.^{13,14}

In order to identify a leading compound against *T. cruzi*, in this work we designed and synthesized sixteen new 4-benzylidene-hydrazide-1*H*-pyrazolo[3,4-*b*]pyridine derivatives (**6**) (Scheme 1). We designed this new series of 1*H*-pyrazolo[3,4-*b*]pyridine derivatives presenting substituent groups with different redox properties in the benzylidene hydrazide moiety possibly analogous to the redox properties of the conventional drugs (benznidazole, allopurinol, and nifurtimox) (Scheme 1). Stereoelectronic properties were also evaluated in the phenyl at 6 position of the pyrazolopyridine heterocycle. Aromatic aldehydes were chosen in a way to explore the contribution of lipophilic and electrophilic properties of these substituents to the biological activity.¹⁵ In addition we tested the precursor of these compounds (**5**), which does not present the benzylidene hydrazide moiety, to analyze its influence in the anti-parasitic profile. The structure–activity relationship study of these compounds was also conducted by comparing the biological effects with the theoretical parameters of the compounds such as HOMO and LUMO (energy, coefficient orbital, and density), GAP and clog*P* calculated by using a molecular modeling approach.

2. Results and discussion

2.1. Chemistry

The synthetic pathway is depicted in Scheme 1. The intermediate compound **4** may be obtained in ~50% yield by a sequence of five reactions as described for ethyl-3-methyl-1-phenyl-1*H*-pyrazolo[3,4-*b*]pyridine-4-carboxylate.¹⁰ This new method explores the commercially available ethyl pyruvate in a modified Quiroga reaction (Scheme 1).¹⁶

Briefly the 5-amino-3-methyl-1-phenyl-1*H*-pyrazole **3** was reacted with aromatic aldehydes and ethyl pyruvate to originate ester **4**, which was confirmed by ¹H NMR (C-5 hydrogen atom = δ8.20 ppm, ester function = δ4.6 and δ1.5 ppm), GC–MS (one peak at 31.93 min) and the fragment *m/z* = 357 (100%) in MS spectrometry. Ester **4** was converted to the hydrazine **5** using a functional group conversion and the treatment with hydrazine hydrate (80%) in ethanol. Derivative **5** showed a characteristic band of –NH group in ν3210–3190 cm^{–1} in the IR spectra. We performed the conversion of **5** to the benzylidene-carbohydrazide **6** by condensation using the appropriate aromatic aldehydes in acidic medium.¹⁷ The IR spectra also showed the carbonyl group of the compounds **6a–6p** in 1650 cm^{–1}.

The presence of a tautomeric enidrazine form was considered¹⁸ but the IR analysis revealed only the hydrazine form with a strong absorption band assigned to group –NH in ν3200 cm^{–1}. The ¹H and ¹³C NMR spectra showed signals in a range of δ 8.3–9.1 ppm and δ 147.1–149.5 ppm corresponding to the methylenic groups (–CH=phenyl).¹⁹ The benzylidene-carbohydrazide unit revealed no characteristic doublet signal in the ¹H and ¹³C NMR spectra, which suggest the existence of a single diastereoisomer. These results suggested that the thermodynamic control favored the formation of a unique diastereoisomeric product in the condensation step among hydrazide (**5**) and different aromatic aldehydes.

2.2. Biology

All compounds in the 1*H*-pyrazolo[3,4-*b*]pyridine series (**6a–6p**) were tested and showed some level of antiparasite activity, except for **6o** derivative (Fig. 2). These data reinforced pyrazolopyridine as a potential system for antiparasite activity as suggested by literature.^{9–12}

Compared to crystal violet (IC₅₀ = 71 μg/mL), and the non-substituted derivative (**6a**) (IC₅₀ = 205.3 μg/mL), the presence of fluorine atom or hydroxyl group at Y position resulted in at least two promising compounds (IC₅₀ < 150 μg/mL) in each set of derivatives (**6b** and **6f**, **6g** and **6i**, respectively) such as nitro group that revealed three compounds (**6l–n**) (Fig. 2 and Table 1). Indeed, among the three substituents used at Y position (F, OH, and NO₂), the better profile was observed with OH (**6g**) (IC₅₀ = 1.9 μg/mL) that exhibited approximately a 35- and 100-fold higher activity than crystal violet and the non-substituted derivative **6a**, respectively (Fig. 2 and Table 1). Despite the chemical features of

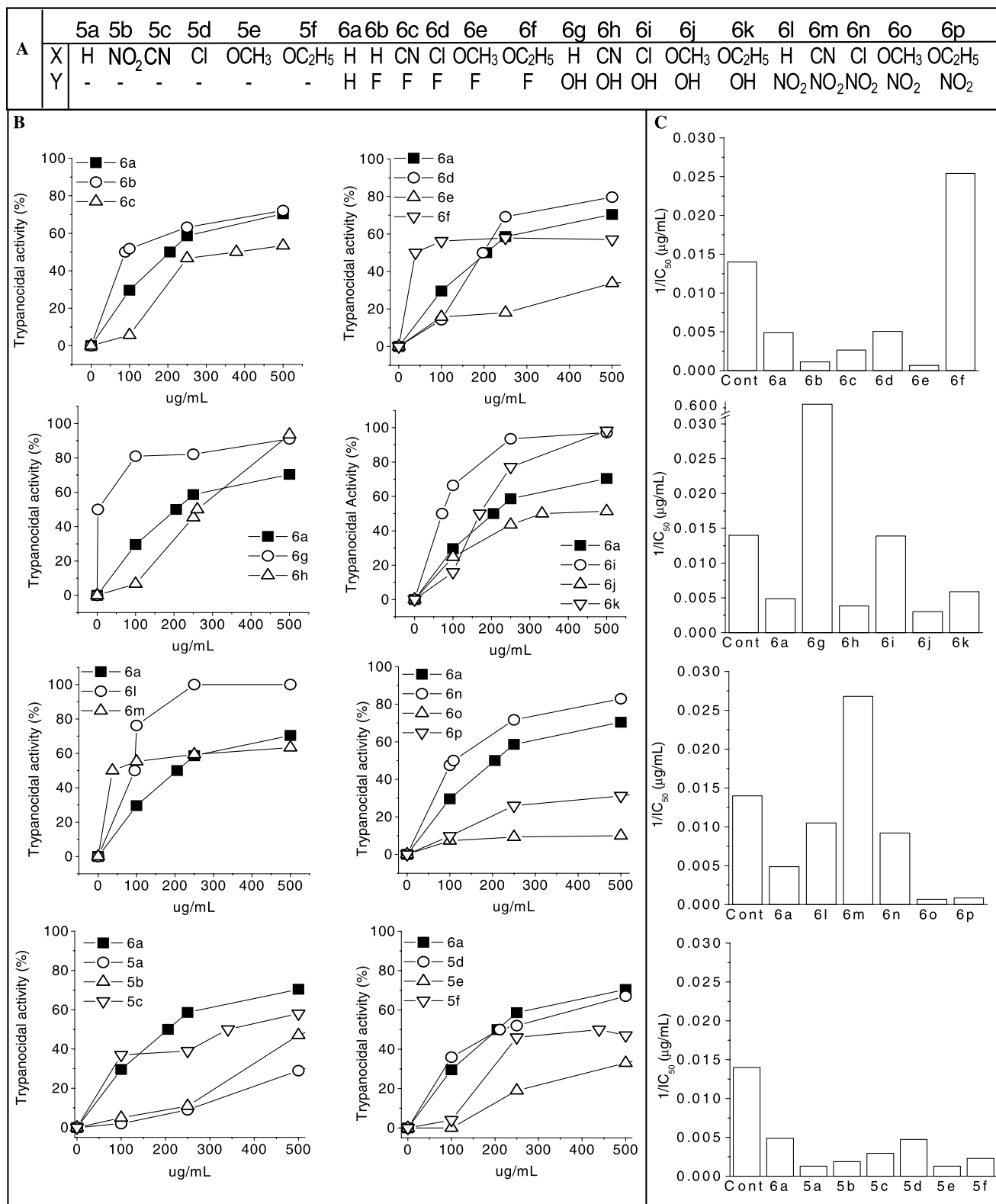


Figure 2. The *N'*-benzylidene-3-methyl-1,6-diphenyl-1*H*-pyrazolo[3,4-*b*]pyridine-4-carbohydrazide (**6a–6p**) and its precursors 3-methyl-1,6-diphenyl-1*H*-pyrazolo[3,4-*b*]pyridine-4-carbohydrazide (**5a–5f**) substituents (A), the in vitro trypanocidal activity (%) (B), and the inhibitory effect (concentration that inhibits 50% of parasite growth—IC₅₀) expressed as 1/IC₅₀ (C). The non-substituted derivative (**6a**) is represented in all graphics as filled square in (B) and control (Cont) is crystal violet in (C).

Y substituents, the methoxy in X decreased the activity of **6e**, **6j**, and **6o**, compared to the non-substituted compound (**6a**) (Fig. 2 and Table 1). In fact, substitution in

X position seems to be critical for the antichagasic profile as suggested by the biological results of **6b**, **6g** and **6l** (the non-substituted derivatives), which were higher

Table 1. Comparison of in vitro trypanocidal activity and the molecular electronic properties (HOMO and LUMO energy, GAP, and clog *P*) of the *N'*-benzylidene-3-methyl-1,6-diphenyl-1*H*-pyrazolo[3,4-*b*]pyridine-4-carbohydrazide (**6a–6p**), and its precursors (**5a–5f**)

Compound	Y	X	IC ₅₀ (μg/mL)	HOMO (eV)	LUMO (eV)	GAP ^a (eV)	clog <i>P</i>
5a	—	H	781.8	−8.15	1.58	9.73	3.09
5b	—	NO ₂	533.3	−8.12	0.98	9.10	3.12
5c	—	CN	341.2	−8.08	1.27	9.35	3.12
5d	—	Cl	211.0	−7.93	1.71	9.64	3.65
5e	—	OCH ₃	781.2	−8.00	1.71	9.71	2.96
5f	—	OC ₂ H ₅	439.4	−7.98	1.73	9.71	3.30
6a	H	H	205.3	−7.87	1.71	9.58	6.24
6b	F	H	88.9	−7.92	1.65	9.57	6.40
6c	F	CN	378.2	−8.15	1.12	9.27	6.43
6d	F	Cl	197.2	−8.01	1.51	9.52	6.96
6e	F	OCH ₃	1461.0	−7.86	1.72	9.58	6.27
6f	F	OC ₂ H ₅	39.3	−7.84	1.75	9.59	6.61
6g	OH	H	1.9	−7.87	1.72	9.59	5.37
6h	OH	CN	260.3	−8.11	1.17	9.28	5.88
6i	OH	Cl	71.8	−7.96	1.56	9.52	6.41
6j	OH	OCH ₃	331.5	−7.82	1.80	9.62	5.73
6k	OH	OC ₂ H ₅	169.6	−7.81	1.81	9.62	6.06
6l	NO ₂	H	95.3	−8.04	0.77	8.81	6.28
6m	NO ₂	CN	37.3	−8.28	0.65	8.93	6.31
6n	NO ₂	Cl	108.5	−8.13	0.73	8.86	6.83
6o	NO ₂	OCH ₃	>1500	−7.97	0.78	8.75	6.15
6p	NO ₂	OC ₂ H ₅	1179.0	−7.96	0.78	8.74	6.48

^a GAP = $E_{\text{LUMO}} - E_{\text{HOMO}}$.

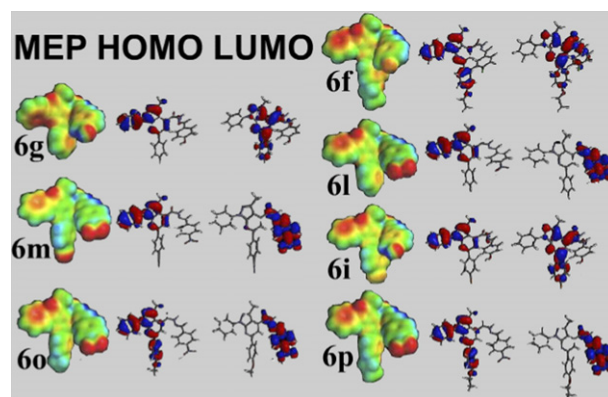
active than those of **6e**, **6j**, and **6o**, the substituted compounds in this position (Fig. 2 and Table 1). The analysis of Table 1 suggested that increments in the atomic size of the substituent in that position could induce a steric effect that may prevent the perfect interaction of the target/receptor.

In order to evaluate the importance of the benzylidene-carbohydrazide, we tested the derivative precursors, which did not present this moiety (**5a–5f**) (Fig. 2). Our experimental data showed that most of these compounds were less active ($\text{IC}_{50} = 341\text{--}781.8\text{ }\mu\text{g/mL}$) than **6a** ($\text{IC}_{50} = 205.3\text{ }\mu\text{g/mL}$), except for **5d**, the chlorine substituted derivative ($\text{IC}_{50} = 211\text{ }\mu\text{g/mL}$) (Fig. 2/Table 1). These data pointed out this region with a significant role for the improvement of the antiparasitic profile.

2.3. SAR studies

Three-dimensional isosurfaces of MEP superimposed onto total electron density of the most representative members ($1000\text{ }\mu\text{g/mL} < \text{IC}_{50} < 50\text{ }\mu\text{g/mL}$) of the 1*H*-pyrazolo[3,4-*b*]pyridine series are presented in Figure 3. The MEP revealed that the negative potential (red region) is present in all three aromatic rings (A, B, and C, see Scheme 1) of the most active compounds (**6g**, **6m**, **6i**, and **6f**) in contrast to the less active (**6o** and **6p**), which presented only two negative regions (Fig. 3).

To gain insight into the atomic contribution on the frontier orbital, we analyzed the three-dimensional HOMO and LUMO coefficient contribution. The study of these compounds showed the HOMO orbital concentrated at A ring in **6g**, **6m**, and **6i**. Differently **6o** and **6p** showed HOMO coefficient orbital distributed along both A and B rings, which may affect their interaction with the target receptor (Fig. 3). Meanwhile LUMO is locat-

**Figure 3.** Comparison of molecular electrostatic potential energy isosurfaces (MEP), HOMO and LUMO orbital coefficients of **6g**, **6f**, **6i**, **6m**, the most active compounds, and **6o** and **6p**, the less active derivatives of 1*H*-pyrazolo[3,4-*b*]pyridine series.

ed between B ring and the pyrazole-pyridine moiety, except when nitro is in Y position (**6m**).

Interestingly, the derivative precursors that do not present the benzylidene-carbohydrazide moiety (**5a–5f**) were poorly active, which infers the requirement of this moiety for a good biological profile. These compounds presented higher GAP values (Table 1), which is the difference between the energies of the frontier orbitals. This feature may have contributed to their smaller activity. In addition the **5a–5f** lowest clog *P* values may be deleterious for their biological activity as it may compromise reaching the target inside the cell by these molecules. This is inferred by **5d** that presents the highest clog *P* and the lowest IC_{50} of this set of compounds.

The individual analysis of the most active compound **6g** suggested that the hydroxyl group might act as a

hydrogen bond donor in the interaction with the receptor. The HOMO density is concentrated on the topside-left of **6g** structure in a higher degree while A ring presents a different orientation compared to **6j**, **6k** and **6o**, some of the less active compounds. These **6g** structural features seem to be important for displaying a significant antiparasitic activity (Fig. 4 and Table 1).

Currently there are many approaches that assess a compound's druglikeness partially based on topological descriptors, fingerprints of molecular drug likeness structure keys or other properties as clog *P* and molecular weights.²⁰ In the Osiris program (<http://www.organic-chemistry.org/prog/peo/>), the occurrence frequency of each fragment is determined within the collection of traded drugs and within the supposedly non-drug-like collection of Fluka compounds. On that case, positive values (0.1–10) point out that the molecule contains predominantly the better fragments, which are frequently present in commercial drugs. In this work we used the Osiris program for calculating the fragment based druglikeness of the most active (**6g**), the inactive compound (**6o**), and some intermediate compounds (**6j** and **6k**) along with nifurtimox and benznidazole, the current toxic antichagasic drugs. Interestingly **6g** (IC₅₀ = 1.9 µg/mL) presented a potential druglikeness value higher than those of the molecules studied including nifurtimox and benznidazole while **6o** presented the lowest value among them (Fig. 4).

In this study we also verified the drug score, which combines druglikeness, clog *P*, log *S*, molecular weight, and

toxicity risks in one value and that may be used to judge the compound's overall potential to qualify for a drug.¹⁸ Our theoretical data showed that **6g** was comparable to benznidazole but better than nifurtimox. Once more **6j** and **6k**, the intermediate compounds and **6o**, the inactive compound, presented lower values in agreement to their biological activity. These results suggested that the structural features of **6g** might be useful in designing new antichagasic agents.

3. Conclusion

In conclusion, we have developed an easy one-step synthesis to obtain the *N'*-benzylidene-3-methyl-1,6-diphenyl-1*H*-pyrazolo[3,4-*b*]pyridine-4-carbohydrazide using a modified Quiroga reaction. The benzylidene-carbohydrazide derivatives (**6**) could be obtained just by using functional group conversions. The **6g** derivative showed the highest trypanocidal profile according to the higher HOMO coefficient orbital and density, which is localized in the A ring, and to its higher druglikeness value compared to other trypanocidal drugs. The biological and SAR results pointed out **6g** as a potential leading compound for the development of new drugs for Chagas treatment.

4. Experimental

4.1. Chemistry

Melting points were determined in a capillary Thomas Hoover apparatus and are given uncorrected. Infrared (IR) spectra were recorded on a Perkin-Elmer 1420 spectrometer in potassium bromide pellets. The ¹H and ¹³C NMR spectra were recorded using a Varian UNITY-plus-300 at 300 MHz spectrophotometer for solutions in DMSO. GC–MS spectra were recorded using a GC 6850N Network, GS system (Agilent), injector 7683 series, detector 5973N, mass selective detector, column: DB-5 ms, 30 m, ID: 0.25 × 0.25 µm. The progress of all reactions was monitored by t.l.c. performed on Kilsiegel 60F 0.2 mm (Merck-Darmstadt). The developed chromatograms were viewed under ultraviolet light (254–365 nm).

4.2. General procedure for the preparation of ethyl 3-methyl-1-phenyl-6-substituted-phenyl-1*H*-pyrazolo[3,4-*b*]pyridine-4-carboxylate (**4a–4f**)

To a solution of aromatic aldehydes (5.78 mmol) in EtOH (15 mL) and 5 drops of hydrochloric acid was added 5-amino-3-methyl-1-phenyl-1*H*-pyrazole (1 g, 5.78 mmol). The reaction mixture was stirred at reflux temperature for 2 h. Then ethyl pyruvate (5.78 mmol) was added and the mixture was kept, at these conditions, for additional 2 h. After cooling to room temperature, the reaction mixture was poured into cold water and 20% aqueous NaOH solution was added to obtain the solid precipitated. The product was filtered off, washed with cold water and dried. Recrystallization from ethanol/water led to ethyl carboxylate derivatives.

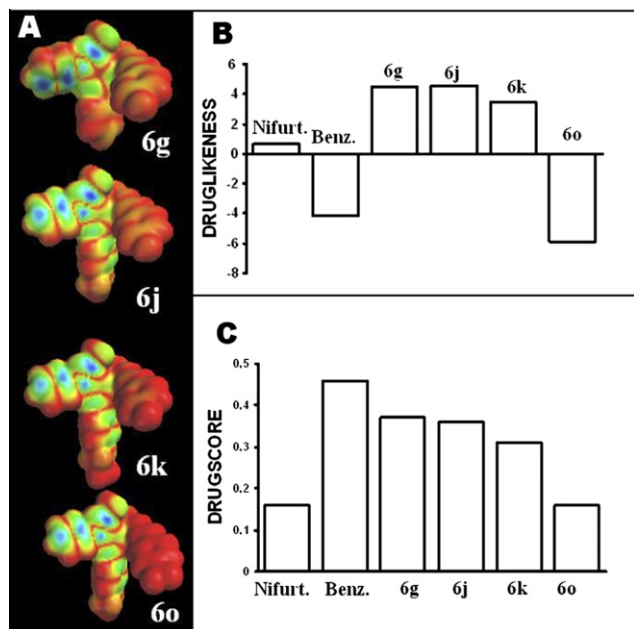


Figure 4. Comparison of **6g**, **6j**, **6k**, and **6o** that vary from the highest to the inactive profile. (A) HOMO density encoded onto a van der Waals surface (isodensity 0.002 e/au³) with the HOMO's absolute density coefficient mapped from deepest red (0.00) to deepest blue (0.03), (B) druglikeness and (C) drugscore values of the **6g**, **6j**, **6k**, and **6o** compared to those of nifurtimox and benznidazole using Osiris program. (<http://www.organic-chemistry.org/prog/peo/druglikeness.html>).

4.2.1. Ethyl 3-methyl-1,6-diphenyl-1H-pyrazolo[3,4-*b*]pyridine-4-carboxylate (4a). 50%, mp = 123 °C. IR (ν -cm⁻¹): 3040 (C–H); 1760 (C=O); 1590–1570 (C=C). GC/MS: rt 31.93 min, area 100%, 357 (100%); 328 (15.78%); 77 (24.45%). ¹HNMR: δ 1.50 (t, 3H, H-11, *J* = 7 Hz); 4.50 (q, 2H, H-10, *J* = 7 Hz); 2.80 (s, 3H, H-8); 8.13 (s, 1H, H-5); 8.35 (dd, 2H, H-2', H-6', *J* = 7.1 Hz, 1.4 Hz); 8.20 (m, 3H, H-3', H-4', H-5'); 7.50 (m, 5H, H-2''–H-5'').

4.2.2. Ethyl 3-methyl-1-phenyl-6-*p*-nitrophenyl-1H-pyrazolo[3,4-*b*]pyridine-4-carboxylate (4b). 50%, mp = 138 °C. IR (ν -cm⁻¹): 2980–2920 (C–H); 1760 (C=O); 1600–1570 (C=C); 1540, 1340 (NO₂). ¹HNMR: δ 1.50 (t, 3H, H-11, *J* = 7.2 Hz); 4.60 (q, 2H, H-10, *J* = 7.2 Hz); 2.00 (s, 3H, H-8); 8.00 (s, 1H, H-5); 8.20 (m, 2H, H-3'', H-5''); 7.90 (m, 2H, H-2'', H-6''); 7.20 (m, 3H, H-3'–H-5'); 7.70 (m, 2H, H-2', H-6').

4.2.3. Ethyl 3-methyl-1-phenyl-6-*p*-cyanophenyl-1H-pyrazolo[3,4-*b*]pyridine-4-carboxylate (4c). 35%, mp = 144 °C. IR (ν -cm⁻¹): 3040–2920 (C–H); 2210 (CN); 1730 (C=O); 1600–1590 (C=C). ¹HNMR: δ 1.50 (t, 3H, H-11, *J* = 7.2 Hz); 4.60 (q, 2H, H-10, *J* = 7.2 Hz); 2.00 (s, 3H, H-8); 8.30 (s, 1H, H-5); 8.46 (d, 2H, H-3'', H-5'', *J* = 8.1 Hz); 8.15 (d, 2H, H-2'', H-6'', *J* = 8.1 Hz); 8.34 (d, 2H, H-2', H-6', *J* = 7.8 Hz); 7.48 (t, 1H, H-4'); 7.75 (t, 2H, H-3', H-5', *J* = 7.8 Hz).

4.2.4. Ethyl 3-methyl-1-phenyl-6-*p*-chlorophenyl-1H-pyrazolo[3,4-*b*]pyridine-4-carboxylate (4d). 44%, mp = 123 °C. IR (ν -cm⁻¹): 3040–2920 (C–H); 1730 (C=O); 1590–1570 (C=C). ¹HNMR: δ 1.50 (t, 3H, H-11, *J* = 7 Hz); 4.60 (q, 2H, H-10, *J* = 7 Hz); 2.00 (s, 3H, H-8); 8.26 (s, 1H, H-5); 7.48 (m, 2H, H-2'', H-6''); 7.72 (m, 2H, H-3'', H-5''); 8.35 (m, 5H, H-2'–H-6').

4.2.5. Ethyl 3-methyl-1-phenyl-6-*p*-methoxyphenyl-1H-pyrazolo[3,4-*b*]pyridine-4-carboxylate (4e). 30%, mp = 122 °C. IR (ν -cm⁻¹): 3040–2920 (C–H); 1760 (C=O); 1610–1570 (C=C). ¹HNMR: δ 1.55 (t, 3H, H-11, *J* = 6.9 Hz); 4.60 (q, 2H, H-10, *J* = 6.9 Hz); 2.00 (s, 3H, H-8); 7.90 (s, 1H, H-5); 4.00 (s, 3H, OCH₃); 7.25 (m, 2H, H-3'', H-5''); 7.48 (m, 2H, H-2'', H-6''); 7.75 (m, 3H, H-3'–H-5'); 8.40 (m, 2H, H-2', H-6').

4.2.6. Ethyl 3-methyl-1-phenyl-6-*p*-ethoxyphenyl-1H-pyrazolo[3,4-*b*]pyridine-4-carboxylate (4f). 30%, mp = 112 °C. IR (ν -cm⁻¹): 2980–2920 (C–H); 1740 (C=O); 1620–1570 (C=C). ¹HNMR: δ 1.45 (t, 3H, H-11, *J* = 6.9 Hz); 4.60 (q, 2H, H-10, *J* = 6.9 Hz); δ 1.60 (t, 3H, OCH₂CH₃, *J* = 7.0 Hz); 4.60 (q, 2H, OCH₂CH₃, *J* = 7.0 Hz); 8.25 (s, 1H, H-5); 7.20 (d, 2H, H-3'', H-5'', *J* = 9 Hz); 8.30 (d, 2H, H-2'', H-6'', *J* = 9 Hz); 8.40 (dd, 2H, H-2', H-6', *J* = 7.5 and 1.2 Hz); 7.70 (m, 2H, H-3', H-5'); 7.50 (m, 1H, H-4').

4.3. General procedure for the preparation of 3-methyl-1-phenyl-6-substituted-phenyl-1H-pyrazolo[3,4-*b*]pyridine-4-carbohydrazide (5a–5f)

Hydrazine monohydrate (1 mL) was added to a solution of **6** (0.56 mmol) in ethanol (5 mL). The reaction mix-

ture was refluxed for 3 h under stirring. After cooling to room temperature, the mixture was added to cold water. The solid precipitated was filtered, washed with water, and dried.

4.3.1. 3-Methyl-1,6-diphenyl-1H-pyrazolo[3,4-*b*]pyridine-4-carbohydrazide (5a). 92%, mp = 200 °C. IR (ν -cm⁻¹): 3300 (N–H); 3200 (N–H); 1650 (C=O); 1500 (C=C). ¹HNMR: δ 2.80 (s, 3H, H-8); 8.13 (s, 1H, H-5); 8.30 (m, 3H, H-3''–H-5''); 7.40 (m, 5H, H-2'–H-6'); 8.00 (m, 2H, H-2'', H-6''); 10.20 (s, 1H, NH); 5.00 (s, 2H, NH₂).

4.3.2. 3-Methyl-1-phenyl-6-*p*-nitrophenyl-1H-pyrazolo[3,4-*b*]pyridine-4-carbohydrazide (5b). 75%, mp = 282 °C. IR (ν -cm⁻¹): 3290 (N–H); 1640 (C=O); 1560, 1340 (NO₂). ¹HNMR: δ 2.80 (s, 3H, H-8); 8.00 (s, 1H, H-5); 8.20 (m, 2H, H-3'', H-5''); 7.90 (m, 2H, H-2'', H-6''); 7.30 (m, 3H, H-3'–H-5'); 7.70 (m, 2H, H-2', H-6').

4.3.3. 3-Methyl-1-phenyl-6-*p*-cyanophenyl-1H-pyrazolo[3,4-*b*]pyridine-4-carbohydrazide (5c). 95%, mp = 258 °C. IR (ν -cm⁻¹): 3290 (N–H); 2210 (CN); 1680 (C=O). ¹HNMR: δ 2.74 (s, 3H, H-8); 4.88 (sl, 2H, NH₂); 10.55 (sl, 1H, NH); 7.72 (dd, 2H, H-3'', *J* = 7.80 Hz); 7.48 (dd, 1H, H-4', *J* = 7.2 Hz); 8.12 (s, 1H, H-5); 8.14 (d, 2H, H-2', *J* = 8.1 Hz); 8.40 (d, 2H, H-3'', *J* = 8.7 Hz); 8.55 (dd, 2H, H-2'', *J* = 8.4 Hz). ¹³CNMR: δ 15.1 (C-8); 113.0 (C-4''); 114.20 (C-3a); 119.3 (CN); 121.4 (C-5 e C-2'); 126.6 (C-4'); 128.8 (C-3' e C-2''); 129.9 (C-3); 133.6 (C-3''); 139.5 (C-4); 140.2 (C-1'); 151.6 (C-7a); 154.7 (C-6); 165.0 (C=O).

4.3.4. 3-Methyl-1-phenyl-6-*p*-chlorophenyl-1H-pyrazolo[3,4-*b*]pyridine-4-carbohydrazide (5d). 75%, mp = 238 °C. IR (ν -cm⁻¹): 3280 (N–H); 1630 (C=O). ¹HNMR: δ 2.74 (s, 3H, H-8); 4.87 (sl, 2H, NH₂); 10.19 (sl, 1H, N–H); 7.47 (dd, 1H, H-4', *J* = 7.2 Hz); 7.70 (d, 2H, H-3'', *J* = 8.4 Hz); 7.75 (d, 2H, H-2'', *J* = 8.7 Hz); 8.03 (s, 1H, H-5); 8.39 (dd, 2H, H-3', *J* = 5.4 Hz); 8.42 (d, 2H, H-2', *J* = 5.4 Hz). ¹³CNMR: δ 14.4 (C-8); 112.8 (C-3a); 120.5 (C-5 e C-2'); 120.6 (C-4'); 129.0 (C-3', C-2'' e C-3''); 129.1 (C-3); 134.9 (C-4''); 136.7 (C-4); 139.3 (C-1''); 142.4 (C-1'); 150.9 (C-7a); 154.7 (C-6); 164.4 (C=O).

4.3.5. 3-Methyl-1-phenyl-6-*p*-methoxyphenyl-1H-pyrazolo[3,4-*b*]pyridine-4-carbohydrazide (5e). 86%, mp = 205 °C. IR (ν -cm⁻¹): 3280 (N–H); 1630 (C=O). ¹HNMR: δ 2.70 (s, 3H, H-8); 3.97 (s, 3H, OCH₃); 4.93 (sl, 2H, NH₂); 10.17 (s, 1H, N–H); 7.24 (d, 2H, H-3'', *J* = 9 Hz); 7.45 (dd, 1H, H-4', *J* = 7.8 Hz); 7.71 (dd, 2H, H-3', *J* = 7.8 Hz); 7.96 (s, 1H, H-5); 8.34 (d, 2H, H-2'', *J* = 9 Hz); 8.44 (d, 2H, H-2, *J* = 7.8 Hz). ¹³CNMR: δ 14.2 (C-8); 55.4 (OCH₃); 112.3 (C-3a); 114.5 (C-3''); 120.5 (C-5 e C-2'); 125.5 (C-4'); 128.9 (C-2''); 129.2 (C-3'); 130.4 (C-1''); 139.1 (C-4); 141.4 (C-1'); 155.9 (C-4''); 151.2 (C-7a); 161.0 (C-6); 164.8 (C=O).

4.3.6. 3-Methyl-1-phenyl-6-*p*-ethoxyphenyl-1H-pyrazolo[3,4-*b*]pyridine-4-carbohydrazide (5f). 70%, mp = 201 °C. IR (ν -cm⁻¹): 3260 (N–H); 1650 (C=O). ¹HNMR: δ 1.49 (t, 3H, OCH₂CH₃); 2.71 (s, 3H, H-8); 4.68 (q, 2H, OCH₂CH₃); 4.86 (sl, 2H, NH₂); 10.14 (sl, 1H,

N–H); 7.22 (d, 2H, H-3'', $J = 9$ Hz); 7.45 (dd, 1H, H-4', $J = 7.5$ Hz); 7.71 (dd, 2H, H-3', $J = 7.5$ Hz); 7.95 (s, 1H, H-5); 8.32 (d, 2H, H-2'', $J = 9$ Hz); 8.44 (d, 2H, H-2'', $J = 7.5$ Hz). ^{13}C NMR: δ 14.3 (C-8); 14.5 (OCH₂CH₃); 63.3 (OCH₂CH₃); 112.2 (C-3a); 114.8 (C-3''); 120.3 (C-2'); 125.4 (C-4'); 128.8 (C-2''); 129.0 (C-3'); 130.2 (C-3); 138.9 (C-1''); 139.1 (C-4); 142.3 (C-1'); 151.1 (C-7a); 155.9 (C-4''); 160.2 (C-6); 164.7 (C=O).

4.4. General procedure for the preparation of *N'*-benzylidene-3-methyl-1-phenyl-6-substituted-phenyl-1*H*-pyrazolo[3,4-*b*]pyridine-4-carbohydrazide (6a–6p)

Aromatic aldehyde (0.3 mmol) and five drops of hydrochloric acid were added to a solution of (5) (0.3 mmol) in absolute ethanol until complete dissolution. The mixture was refluxed under stirring and the end of reaction monitored by t.l.c. The resulting solution was concentrated under reduced pressure and added cold water. The precipitated was filtered off, washed with cold water, and dried. Recrystallization from ethanol/water led to the expected compounds as colored solids.

4.4.1. *N'*-(Benzylidene)-3-methyl-1,6-diphenyl-1*H*-pyrazolo[3,4-*b*]pyridine-4-carbohydrazide (6a). 98%, mp = 148–150 °C. IR ($\nu\text{-cm}^{-1}$): 1650 (C=O); 3190 (N–H). ^1H NMR: δ 2.70 (s, 3H, H-8); 8.20 (s, 1H, H-5); 12.40 (s, 1H, H-10); 7.60–7.80 (m, 5H, H-2''–H-6''); 8.10 (s, 1H, H-12); 7.40–7.50 (m, 5H, H-2'–H-6'); 8.40–8.50 (m, 2H, H-2'', H-6''); 7.90 (m, 3H, H-3''–H-5''). ^{13}C NMR: δ 14.4 (C-8); 111 (C-3a); 120.3 (C-5); 120.5 (C-2', C-3'); 129.0 (C-2'', C-3''', C-3'', C-5'', C-3', C-5'); 127.0 (C-2'', C-6''); 130.0 (C-4'''); 133 (C-1''); 134.0 (C-1'); 143 (C-3); 111.0 (C-3a); 161 (C=O); 155.8 (C-6); 151.0 (C-7a); 145.0 (CH-Ar); 141 (C-1'); 130.0 (C-1'').

4.4.2. *N'*-(4-Fluorobenzylidene)-3-methyl-1,6-diphenyl-1*H*-pyrazolo[3,4-*b*]pyridine-4-carbohydrazide (6b). 90%, mp = 284 °C. IR ($\nu\text{-cm}^{-1}$): 3200 (N–H); 1650 (C=O). ^1H NMR: δ 2.70 (s, 3H, H-8); 8.30 (s, 1H, H-5); 12.30 (s, 1H, H-10); 8.10 (s, 1H, H-12); 7.50 (m, 2H, H-3''', H-5'''); 8.40 (m, 5H, H-2''–H-6''); 7.70 (m, 5H, H-2'–H-6'); 8.00 (2H, H-2'', H-6''). ^{13}C NMR: δ 14.2 (C-8); 143.0 (C-3); 156.0 (C-6); 161.5 (C=O); 143.3 (C-1'); 164.5 (C-4'''); 115.6 (C-3a); 138.5 (C-4); 120.0 (C-5); 151.0 (C-7a); 147.9 (CH-Ar).

4.4.3. *N'*-(4-Fluorobenzylidene)-3-methyl-1-phenyl-6-*p*-cyanophenyl-1*H*-pyrazolo[3,4-*b*]pyridine-4-carbohydrazide (6c). 92%, mp = 276–278 °C. IR ($\nu\text{-cm}^{-1}$): 3290 (N–H); 2220 (CN); 1650 (C=O). ^1H NMR: δ 2.74 (s, 3H, H-8); 7.22 (dd, 1H, H-4', $J = 8.7$ Hz); 7.45–7.52 (m, 2H, H-3'); 7.73 (dd, 2H, H-3'', $J = 8.4$ Hz); 7.96–8.01 (m, 2H, H-3''); 8.17 (d, 2H, H-2'', $J = 8.7$ Hz); 8.35 (s, 1H, H-5); 8.41 (d, 2H, H-2'', $J = 9$ Hz); 8.54 (s, 1H, H-12); 12.43 (sl, 1H, H-10). ^{13}C NMR: δ 14.4 (C-8); 112.3 (C-3a e C-4''); 113.2 (C-3'''); 118.6 (CN); 120.5 (C-5 e C-2'); 125.8 (C-4'); 128.0 (C-2'''); 129.3 (C-3'); 130.5 (C-3); 138.7 (C-1'''); 140.0 (C-4); 141.8 (C-1''); 142.0 (C-1'); 148.0 (C-12); 150.9 (C-7a); 153.8 (C-6); 161.4 (C-4'''); 165.0 (C=O).

4.4.4. *N'*-(4-Fluorobenzylidene)-3-methyl-1-phenyl-6-*p*-chlorophenyl-1*H*-pyrazolo[3,4-*b*]pyridine-4-carbohydrazide (6d). 93%, mp = 230 °C. IR ($\nu\text{-cm}^{-1}$): 3260 (N–H); 1650 (C=O). ^1H NMR: δ 2.73 (s, 3H, H-8); 7.18–7.24 (m, 1H, H-4'); 7.41–7.51 (m, 2H, H-3'); 7.69 (d, 2H, H-3'', $J = 8.4$ Hz); 7.73–7.77 (m, 2H, H-3'''); 7.96–7.99 (m, 2H, H-2'''); 8.20 (s, 1H, H-5); 8.36–8.44 (m, 4H, H-2' e H-2''); 8.45 (s, 1H, H-12); 12.31 (sl, 1H, H-10). ^{13}C NMR: δ 14.2 (C-8); 111.9 (C-3a); 112.7 (C-3'''); 120.4 (C-5 e C-2'); 125.5 (C-4'); 128.9 (C-2'' e C-2'''); 129.0 (C-3''); 129.4 (C-3'); 130.5 (C-3); 134.8 (C-1'''); 136.7 (C-4''); 138.9 (C-4); 139.2 (C-1''); 142.3 (C-1'); 148.0 (C-12); 150.9 (C-7a); 154.7 (C-6); 161.5 (C-4'''); 164.4 (C=O).

4.4.5. *N'*-(4-Fluorobenzylidene)-3-methyl-1-phenyl-6-*p*-methoxyphenyl-1*H*-pyrazolo[3,4-*b*]pyridine-4-carbohydrazide (6e). 94%, mp = 264 °C. IR ($\nu\text{-cm}^{-1}$): 3560 (N–H); 1650 (C=O); 1350 (C–O–C). ^1H NMR: δ 2.71 (s, 2H, H-8); 3.97 (s, 3H, OCH₃); 7.25 (dd, 1H, H-4', $J = 8.7$ Hz); 7.43–7.48 (m, 2H, H-3'''); 7.69–7.75 (m, 4H, H-3' e H-2''); 7.95–8.00 (m, 2H, H-3''); 8.18 (s, 1H, H-5); 8.34 (d, 2H, H-2'', $J = 9$ Hz); 8.44 (d, 2H, H-2', $J = 8.7$ Hz); 8.54 (s, 1H, H-12); 12.38 (sl, 1H, H-10). ^{13}C NMR: δ 14.2 (C-8); 55.2 (OCH₃); 111.1 (C-3a); 112.1 (C-3'''); 114.2 (C-3''); 120.5 (C-5 e C-2'); 125.3 (C-4'); 128.7 (C-2'' e C-3'); 128.9 (C-2'''); 130.3 (C-3); 138.9 (C-4 e C-1''); 142.2 (C-1'); 152.2 (C-7a); 155.8 (C-6 e C-4''); 160.8 (C-4'''); 164.5 (C=O).

4.4.6. *N'*-(4-Fluorobenzylidene)-3-methyl-1-phenyl-6-*p*-ethoxyphenyl-1*H*-pyrazolo[3,4-*b*]pyridine-4-carbohydrazide (6f). 83%, mp = 190 °C. IR ($\nu\text{-cm}^{-1}$): 3240–3200 (N–H); 1650 (C=O). ^1H NMR: δ 1.50 (t, 3H, OCH₂CH₃); 2.72 (s, 3H, H-8); 4.24 (q, 2H, OCH₂CH₃); 7.21 (d, 2H, H-3'', $J = 8.7$ Hz); 7.46 (d, 1H, H-4', $J = 6.3$ Hz); 7.68–7.73 (m, 6H, H-3', H-3'', H-2''); 7.94 (s, 1H, H-5); 8.31 (d, 2H, H-2'', $J = 8.7$ Hz); 8.44 (d, 2H, H-2', $J = 7.8$ Hz); 12.30 (sl, 1H, H-10). ^{13}C NMR: δ 14.3 (C-8); 14.5 (OCH₂CH₃); 63.2 (OCH₂CH₃); 111.2 (C-3a); 112.2 (C-3'''); 114.8 (C-3''); 120.3 (C-5 e C-2'); 125.4 (C-4'); 128.7 (C-2''); 129.0 (C-3'); 130.0 (C-3); 138.4 (C-1'''); 138.9 (C-1''); 139.1 (C-4); 142.3 (C-1'); 147.9 (C-12); 151.1 (C-7a); 155.8 (C-4''); 160.2 (C-4'''); 161.8 (C-6); 164.8 (C=O).

4.4.7. *N'*-(4-Hydroxybenzylidene)-3-methyl-1,6-diphenyl-1*H*-pyrazolo[3,4-*b*]pyridine-4-carbohydrazide (6g). 97%, mp = 278–280 °C. IR ($\nu\text{-cm}^{-1}$): 3300–3100 (OH); 1660 (C=O). ^1H NMR: δ 2.73 (s, 3H, H-8); 8.20 (s, 1H, H-5); 12.10 (s, 1H, H-10); 10.00 (s, 1H, H-12); 6.80 (d, 2H, H-3''', H-5''', $J = 9$ Hz); 7.35 (d, 2H, H-2''', H-6''', $J = 9$ Hz); 7.50 (m, 3H, H-3''–H-5''); 7.60–7.80 (m, 7H, H-2'–H-6', H-2'', H-6''); 8.10 (s, 1H, OH). ^{13}C NMR: δ 15.6 (C-8); 144.0 (C-3); 156 (C-6); 163.0 (C=O); 140 (C-1'); 151.0 (C-7a); 143.0 (CH-Ar); 160.0 (C-4'''); 120.0 (C-5); 111.0 (C-3a).

4.4.8. *N'*-(4-Hydroxybenzylidene)-3-methyl-1-phenyl-6-*p*-cyanophenyl-1*H*-pyrazolo[3,4-*b*]pyridine-4-carbohydrazide (6h). 65%, mp = 278 °C. IR ($\nu\text{-cm}^{-1}$): 3500–3200 (OH); 2220 (CN); 1650 (C=O). ^1H NMR: δ 2.72 (s, 3H, H-8); 6.99 (d, 2H, H-3''', $J = 7.5$ Hz); 7.46 (dd, 1H, H-4', $J = 7.2$ Hz); 7.69 (d, 2H, H-3', $J = 7.2$ Hz);

7.74 (d, 2H, H-3'', $J = 8.7$ Hz); 8.11 (d, 2H, H-2'', $J = 8.1$ Hz); 8.28 (s, 1H, H-5); 8.38 (d, 2H, H-2'', $J = 8.4$ Hz); 8.43 (s, 1H, H-12); 8.54 (d, 2H, H-2', $J = 7.2$ Hz); 10.13 (s, 1H, OH); 12.17 (sl, 1H, H-10). ^{13}C NMR: δ 14.4 (C-8); 112.3 (C-3a e C-4''); 118.6 (CN); 120.7 (C-5 e C-2'); 124.9 (C-3); 125.7 (C-4'); 128.4 (C-3'); 129.2 (C-2''); 132.8 (C-3''); 138.8 (C-1'''); 139.1 (C-4); 140.2 (C-1'); 141.9 (C-1''); 149.5 (C-12); 150.8 (C-7a); 153.7 (C-4'''); 159.8 (C-6); 161.1 (C=O).

4.4.9. *N'*-(4-Hydroxybenzylidene)-3-methyl-1-phenyl-6-*p*-chlorophenyl-1*H*-pyrazolo[3,4-*b*]pyridine-4-carbohydrazide (6i). 73%, mp = >310 °C. IR ($\nu\text{-cm}^{-1}$): 3400–3220 (OH); 1650 (C=O). ^1H NMR: δ 2.72 (s, 3H, H-8); 6.76 (d, 2H, H-3''', $J = 8.7$ Hz); 7.25 (d, 2H, H-2'', $J = 8.4$ Hz); 7.46 (dd, 1H, H-4', $J = 7.5$ Hz); 7.69–7.76 (m, 2H, H-3'); 7.76–7.89 (m, 2H, H-3''); 8.20 (s, 1H, H-5); 8.31–8.37 (m, 2H, H-2''); 8.40 (d, 2H, H-2', $J = 8.7$ Hz); 8.46 (s, 1H, H-12); 10.08 (s, 1H, OH); 12.12 (sl, 1H, H-10). ^{13}C NMR: δ 14.4 (C-8); 11.9 (C-3a); 115.8 (C-3'''); 120.4 (C-5); 120.6 (C-2'); 124.9 (C-3); 125.8 (C-2''); 129.0 (C-3''); 129.2 (C-3'); 135.0 (C-1'''); 136.6 (C-4''); 139.0 (C-4); 140.1 (C-1''); 142.3 (C-1'); 149.4 (C-12); 151.0 (C-7a); 154.9 (C-6); 159.8 (C-4'''); 161.3 (C=O).

4.4.10. *N'*-(4-Hydroxybenzylidene)-3-methyl-1-phenyl-6-*p*-methoxyphenyl-1*H*-pyrazolo[3,4-*b*]pyridine-4-carbohydrazide (6j). 88%, mp = 270 °C. IR ($\nu\text{-cm}^{-1}$): 3300–3220 (OH); 1650 (C=O). ^1H NMR: δ 2.71 (s, 3H, H-8); 3.77 (s, 3H, OCH₃); 6.99 (d, 2H, H-3''', $J = 8.4$ Hz); 7.20–7.27 (m, 2H, H-3'); 7.46 (dd, 1H, H-4', $J = 8.7$ Hz); 7.70 (d, 2H, H-2'', $J = 8.4$ Hz); 7.75 (d, 2H, H-3'', $J = 8.7$ Hz); 8.14 (s, 1H, H-5); 8.38 (d, 2H, H-2'', $J = 9$ Hz); 8.43 (s, 1H, H-12); 8.45 (d, 2H, H-2', $J = 7.5$ Hz); 10.12 (s, 1H, OH); 12.14 (sl, 1H, H-10). ^{13}C NMR: δ 14.4 (C-8); 55.4 (OCH₃); 111.2 (C-3a); 114.5 (C-3''); 115.7 (C-3'''); 120.5 (C-5 e C-2'); 124.9 (C-3); 125.6 (C-4'); 128.5 (C-2'''); 129.0 (C-2''); 129.2 (C-3'); 130.2 (C-3'); 138.8 (C-4); 139.1 (C-1''); 142.2 (C-1'); 149.3 (C-12); 151.1 (C-7a); 156.0 (C-4'''); 159.8 (C-4''); 161.0 (C-6); 161.5 (C=O).

4.4.11. *N'*-(4-Hydroxybenzylidene)-3-methyl-1-phenyl-6-*p*-ethoxyphenyl-1*H*-pyrazolo[3,4-*b*]pyridine-4-carbohydrazide (6k). 92%, mp = 288–290 °C. IR ($\nu\text{-cm}^{-1}$): 3400–3200 (OH); 1660 (C=O). ^1H NMR: δ 1.47 (t, 3H, OCH₂CH₃); 2.87 (s, 3H, H-8); 4.66 (q, 2H, OCH₂CH₃); 7.51 (d, 2H, H-3''', $J = 8.4$ Hz); 7.73 (d, 2H, H-2'', $J = 8.4$ Hz); 7.97 (d, 1H, H-4', $J = 7.5$ Hz); 8.21 (d, 2H, H-3', $J = 8.1$ Hz); 8.26 (d, 2H, H-3''', $J = 8.4$ Hz); 8.65 (s, 1H, H-5); 8.87–8.96 (m, 2H, H-2'); 8.89 (d, 2H, H-2'', $J = 8.7$ Hz); 8.99 (s, 1H, H-12); 10.62 (s, 1H, OH); 12.35 (sl, 1H, H-10). ^{13}C NMR: δ 14.4 (C-8); 14.5 (OCH₂CH₃); 63.3 (OCH₂CH₃); 11.2 (C-3a); 115.6 (C-3'''); 120.1 (C-2'); 120.4 (C-5); 124.9 (C-3); 125.5 (C-4'); 127.7 (C-2'''); 128.7 (C-2''); 129.1 (C-3'); 130.0 (C-1''); 138.7 (C-1'''); 139.1 (C-4); 141.7 (C-1'); 149.2 (C-12); 151.1 (C-7a); 156.0 (C-4'''); 160.3 (C-6); 161.4 (C=O).

4.4.12. *N'*-(4-Nitrobenzylidene)-3-methyl-1,6-diphenyl-1*H*-pyrazolo[3,4-*b*]pyridine-4-carbohydrazide (6l). 78%, mp = 300 °C. IR ($\nu\text{-cm}^{-1}$): 3200 (N–H); 1650 (C=O);

1540 (NO₂). ^1H NMR: δ 2.80 (s, 3H, H-8); 8.30 (s, 1H, H-5); 8.60 (s, 1H, H-12); 12.60 (s, 1H, H-10); 8.40–8.50 (m, 4H, H-2''', H-6'', H-2'', H-6''); 8.20 (m, 2H, H-3'', H-5''); 7.60–7.80 (m, 8H, H-2'–H-6', H-3'–H-5'). ^{13}C NMR: δ 14.2 (C-8); 146.0 (C-3); 156.2 (C-6); 151.1 (C-7a); 161.9 (C=O); 143 (CH-Ar); 141.7 (C-1'); 141.0 (C-1''); 146.0 (C-4''').

4.4.13. *N'*-(4-Nitrobenzylidene)-3-methyl-1-phenyl-6-*p*-cyanophenyl-1*H*-pyrazolo[3,4-*b*]pyridine-4-carbohydrazide (6m). 95%, mp = 305 °C. IR ($\nu\text{-cm}^{-1}$): 3220–3190 (N–H); 2220 (CN); 1660 (C=O); 1540 (NO₂). ^1H NMR: δ 3.23 (s, 3H, H-8); 7.96–8.02 (m, 1H, H-4'); 8.14–8.17 (m, 2H, H-3'''); 8.14–8.26 (m, 2H, H-3'); 8.62–8.69 (m, 2H, H-3''); 8.73–8.78 (m, 2H, H-2''); 8.89 (s, 1H, H-5); 8.90–8.96 (m, 2H, H-2''); 9.06–9.11 (m, 2H, H-2'); 9.12 (s, 1H, H-12); 13.23 (sl, 1H, H-10). ^{13}C NMR: δ 14.3 (C-8); 112.3 (C-4''); 113.7 (C-3a); 120.5 (C-5 e C-2'); 124.1 (C-3'''); 126.1 (C-3); 127.7 (C-4'); 128.2 (C-2''); 128.4 (C-2'''); 129.3 (C-3'); 133.0 (C-3''); 138.8 (C-1''); 139.5 (C-4); 141.8 (C-1''); 143.4 (C-1'); 146.7 (C-12); 148.2 (C-4'''); 150.9 (C-7a); 153.8 (C-6); 161.0 (C=O).

4.4.14. *N'*-(4-Nitrobenzylidene)-3-methyl-1-phenyl-6-*p*-chlorophenyl-1*H*-pyrazolo[3,4-*b*]pyridine-4-carbohydrazide (6n). 97%, mp = 296–298 °C. IR ($\nu\text{-cm}^{-1}$): 3220–3190 (N–H); 1660 (C=O). ^1H NMR: δ 3.23 (s, 3H, H-8); 7.98 (dd, 1H, H-4', $J = 7.5$ Hz); 8.16 (d, 2H, H-3''', $J = 8.7$ Hz); 8.22 (dd, 2H, H-3', $J = 8.1$ Hz); 8.27 (d, 2H, H-2''', $J = 8.7$ Hz); 8.66–8.70 (m, 2H, H-3''); 8.80 (s, 1H, H-5); 8.90–8.96 (m, 4H, H-2' e H-2''); 9.12 (s, 1H, H-12). ^{13}C NMR: δ 14.2 (C-8); 112.2 (C-3a); 120.6 (C-5 e C-2'); 123.8 (C-4'); 127.5 (C-2'''); 128.9 (C-3'); 129.0 (C-3); 132.7 (C-4''); 138.4 (C-4); 138.6 (C-1''); 140.0 (C-1''); 142.1 (C-1'); 146.7 (C-12); 148.1 (C-4'''); 150.1 (C-7a); 154.0 (C-6); 161.6 (C=O).

4.4.15. *N'*-(4-Nitrobenzylidene)-3-methyl-1-phenyl-6-*p*-methoxyphenyl-1*H*-pyrazolo[3,4-*b*]pyridine-4-carbohydrazide (6o). 98%, mp = 284 °C. IR ($\nu\text{-cm}^{-1}$): 3220 (N–H); 1660 (C=O); 1540 (NO₂). ^1H NMR: δ 2.72 (s, 3H, H-8); 3.98 (s, 3H, OCH₃); 7.21–7.27 (m, 2H, H-3'); 7.45–7.50 (m, 1H, H-4'); 7.57–7.65 (m, 4H, H-3' e H-2'''); 8.06–8.21 (m, 2H, H-3''); 8.16 (s, 1H, H-5); 8.36–8.46 (m, 4H, H-2' e H-2''); 8.64 (s, 1H, H-12); 12.66 (sl, 1H, H-10). ^{13}C NMR: δ 14.3 (C-8); 55.3 (OCH₃); 112.6 (C-3a); 114.4 (C-3''); 120.4 (C-5 e C-2'); 123.9 (C-3'''); 125.5 (C-4'); 127.5 (C-2'''); 128.2 (C-2''); 128.9 (C-3'); 130.2 (C-3); 138.0 (C-4); 139.0 (C-1''); 139.8 (C-1'''); 143.1 (C-1'); 146.6 (C-12); 148.1 (C-4'''); 151.1 (C-7a); 155.7 (C-4''); 161.0 (C-6); 162.1 (C=O).

4.4.16. *N'*-(4-Nitrobenzylidene)-3-methyl-1-phenyl-6-*p*-ethoxyphenyl-1*H*-pyrazolo[3,4-*b*]pyridine-4-carbohydrazide (6p). 94%, mp = 280–282 °C. IR ($\nu\text{-cm}^{-1}$): 3240–3200 (N–H); 1650 (C=O); 1540 (NO₂). ^1H NMR: δ 1.49 (t, 3H, OCH₂CH₃); 2.72 (s, 3H, H-8); 4.26 (q, 2H, OCH₂CH₃); 7.24 (d, 2H, H-3''', $J = 8.7$ Hz); 7.49 (d, 1H, H-4', $J = 7.5$ Hz); 7.71 (d, 2H, H-2''), 7.74 (d, 2H, H-3', $J = 7.5$ Hz); 8.18 (d, 2H, H-3'', $J = 9$ Hz); 8.20 (s, 1H, H-5); 8.38 (d, 2H, H-2'', $J = 8.7$ Hz); 8.45 (d, 2H, H-2', $J = 8.7$ Hz); 8.64 (s, 1H, H-12); 12.63 (sl, 1H, H-

10). ^{13}C NMR: δ 14.2 (C-8); 14.3 (OCH_2CH_3); 63.2 (OCH_2CH_3); 110.9 (C-3a); 114.8 (C-3''); 120.5 (C-5 e C-2'); 125.5 (C-4'); 128.1 (C-2'''); 128.9 (C-2''); 129.3 (C-3'); 129.9 (C-3); 137.9 (C-1''); 138.9 (C-4); 140.1 (C-1'''); 141.9 (C-1'); 146.4 (C-12); 148.1 (C-1''' e C-4'''); 151.1 (C-7a); 155.9 (C-4''); 160.2 (C-6); 162.0 (C=O).

4.5. Pharmacology

Bloodstream forms were obtained at the peak of parasitaemia (7th day of infection) from albino mice infected with Y strain of *T. cruzi* by cardiac puncture. The infected blood was diluted with blood from healthy mice and fetal bovine serum, in a way to obtain a final parasite concentration of about 106 trypomastigotes forms/mL. Stock solution of the substances was prepared in dimethylsulfoxide (DMSO). Parts of these stock solutions were added to the infected blood in order to obtain final concentrations of 10, 100, 250, 500, and 1000 $\mu\text{g/mL}$ using microplates (96 wheels). The solutions were incubated at 4 °C for 24 h under constant shaking. Untreated and crystal violet treated parasites were used as controls. All assays were performed in triplicate. The activity was determined by counting the trypomastigote forms and determination of parasitical lyses (%) compared to the non-treated control group.²¹ The compound concentration corresponding to 50% activity was expressed as the IC_{50} .

4.6. Molecular modeling

All computations were performed using SPARTAN'04 (Wavefunction Inc., Irvine, CA, 2000) as described elsewhere.²² The conformational analysis of the unsubstituted compound revealed the Syn conformation as the most stable due to an antiparallel dipole of the carbonyl and the NH of the amide moiety. Thus this conformation was used in all theoretical derivatives analysis.

In order to evaluate the electronic properties of all compounds, we submitted them to a Single-Point ab initio calculation with a 6-31G* basis set available on SPARTAN'04 program (Wavefunction Inc., Irvine, CA, 2000). Molecular electrostatic potential maps (MEPs), HOMO and LUMO eigenvalues and orbital coefficients, GAP, and the clogP were calculated. In this work, we generated the MEPs isoenergy contours in a range from -25.000 to $+40.000$ kcal/mol and superimposed onto a surface of constant electron density of $0.002 \text{ e}/\text{au}^3$. HOMO density encoded onto a van der Waals surface (isodensity $0.002 \text{ e}/\text{au}^3$) with the HOMO's absolute density coefficient mapped from deepest red (0.00) to deepest blue (0.03). The constants employed in these isosurface calculations are default parameters in the program used. Theoretical logP (clogP) was calculated using Villar method, at AM1 semiempirical level.

Acknowledgments

We thank Fundação de Amparo à Pesquisa do Estado do Rio de Janeiro (FAPERJ—Brazil) for supporting this research and to Conselho Nacional de Desenvolvimento Científico e Tecnológico (CNPq—Brazil) for fellowships (M.B.S. and A.C.C.F.). We thank Edson F. da Silva for technical support. We would like to extend special thanks to Dr. Mishbaul A. Khan for helpful advice.

References and notes

- Urbina, J. A.; Docampo, R. *Trends Parasitol.* **2003**, *19*, 495.
- Williams-Blangero, S.; VandeBerg, J. L.; Blangero, J.; Correa-Oliveira, R. *Front. Biosci.* **2003**, *8*, 337.
- World Health Organization (WHO). <http://www.who.int/ctd/chagas/index.htm/> Accessed in 2006.
- Dias, J. C.; Silveira, A. C.; Schofield, C. J. *Mem. Inst. Oswaldo Cruz* **2002**, *97*, 603.
- Urbina, J. A. *Curr. Opin. Infect. Dis.* **2001**, *14*, 733.
- Maya, J. D.; Bollo, S.; Nuñez-Vergara, L. J.; Squeella, J. A.; Repetto, Y.; Morillo, A.; Perie, J.; Chauviere, G. *Biochem. Pharmacol.* **2003**, *65*, 999.
- Sosa-Estani, S.; Armenti, A.; Araujo, G.; Viotti, R.; Lococo, B.; Ruiz, V. B.; Vigliano, C.; de Rissio, A. M.; Segura, E. L. *Medicina (B Aires)* **2004**, *64*, 1.
- Reyes, P. A.; Vallejo, M. *Cochrane Database Syst. Rev.* **2005**, *19*, 102.
- Dias, L. R. S.; Nanayakkara, D.; Mcchesney, J. D.; Freitas, A. C. C.; Barreiro, E. J. *Boll. Chim. Farm.* **1997**, *136*, 97.
- Dias, L. R. S.; Freitas, A. C. C.; Barreiro, E. J.; Goins, D. K.; Nanayakkara, D.; Mcchesney, J. D. *Boll. Chim. Farm.* **2000**, *139*, 14.
- Wernsdorfer, W. H.; Allmendinger, T. *IDrugs* **2001**, *4*, 443.
- deMello, H.; Echevarria, A.; Bernardino, A. M.; Canto-Cavalheiro, M.; Leon, L. L. *J. Med. Chem.* **2004**, *47*, 5427.
- Rodrigues, C. R.; Flaherty, T. M.; Springer, C.; McKerrrow, J. H.; Cohen, F. E. *Bioorg. Med. Chem. Lett.* **2002**, *3*, 1537.
- Bernardino, A. M. R.; Gomes, A. O.; Machado, G. M. C.; Canto-Cavalheiro, M. M.; Leon, L. L.; Amaral, V.; Charret, K. S.; Freitas, A. C. C. *Eur. J. Med. Chem.* **2006**, *41*, 80.
- Canto-Cavalheiro, M. M.; Echevarria, A.; Araujo, C. A.; Bravo, M. F.; Santos, L. H.; Jansen, A. M.; Leon, L. L. *Microbios* **1997**, *90*, 51.
- Quiroga, J.; Insuasty, B.; Cruz, S.; Hernandez, P.; Bolanos, A.; Moreno, R.; Hormaza, A.; de Almeida, R. H. S. *J. Heterocycl. Chem.* **1998**, *35*, 333.
- Khan, M. A.; Freitas, A. C. C. *J. Heterocycl. Chem.* **1983**, *20*, 277.
- Szileigyl, G. *Arzneim.—Forsch.* **1984**, *35*, 1260.
- Lynch, B. M.; Khan, M. A.; Teo, H. C.; Pedrotti, F. *Can. J. Chem.* **1988**, *66*, 420.
- Tetko, I. V. *Drug Discov. Today* **2005**, *10*, 22.
- Brener, Z. *Rev. Inst. Med. Trop. Sao Paulo* **1962**, *4*, 389.
- Ferreira, V. F.; Jorquera, A.; Souza, A. M.; da Silva, M. N.; de Souza, M. C.; Gouvea, R. M.; Rodrigues, C. R.; Pinto, A. V.; Castro, H. C.; Santos, D. O.; Araújo, H. P.; Bourguignon, S. C. *Bioorg. Med. Chem.* **2006**, *14*, 5459.